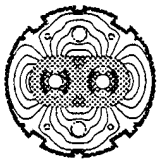

LHC Project Note 15

1995-11-08
(Sgobba@MT.MSM.cem.ch)

TIG Weldability of special Stainless Steels for the Beam Screen of the Large Hadron Collider

J.P. Bacher* and S. Sgobba*

Summary

The Large Hadron Collider (LHC) planned at CERN should operate at cryogenic temperatures (1.9 K) and provide collisions between protons belonging to two beams of 7 TeV of energy each. A "beam screen" cooling at 10 K, intercepting the synchrotron radiation emitted by the circulating protons and the power dissipated by the beam image currents, is designed to shield the magnet cold bore. The screen will be kept during machine operation at temperatures higher than 1.9 K, in order to absorb the heat load at a lower cost. However it must be able to withstand without risk of embrittlement cooling to the magnet temperature of 1.9 K. Any ductile-fragile transition should therefore be avoided down to 1.9 K. Moreover, the screen should be totally amagnetic at cryogenic temperatures (the maximum admitted magnetic susceptibility is 5.10^{-3}). Severe conditions are imposed on the construction material of the beam screen. A quench (sudden loss of superconductivity in the magnet) will induce eddy currents in the screen which result in a risk of plastic deformation. During its life, the screen will be subjected to several thermal cycles between room temperature and cryogenic temperatures.

In the present design, the screen should have a section of 38 x 38 mm^2 and a length of about 15 m and should be longitudinally welded. To avoid a loss of magnetic and mechanical properties at low temperature, no local precipitation of the ferrite in the weld metal and in the Heat Affected Zones (HAZ) should occur. Because of their weldability and excellent austenitic stability, N_2-enriched austenitic stainless steels with different Mn contents are candidate materials for the beam screen. High Mn steels are magnetically stable at low temperature.

The TIG weldability of the candidate steels is studied. The influence of welding parameters (weld speed, power ..) on the possible precipitation of delta ferrite is discussed.

Paper presented at the "34èmes journées du Cercle d'Etude des Métaux". St-Etienne (F), 4-5 May 1995, and published in the Bulletin du Cercle d'Etude des Métaux XVI 10 (May 1995), page 13.1 ff.

* CERN, MT-SM, CH-1211 Geneva, Switzerland

J.P. BACHER* AND S. SGOBBA*

TIG WELDABILITY OF SPECIAL STAINLESS STEELS FOR THE BEAM SCREEN OF THE LARGE HADRON COLLIDER

I- INTRODUCTION

The Large Hadron Collider (LHC) planned at CERN should operate at cryogenic temperatures (1.9 K) and provide collisions between protons belonging to two beams of 7 TeV of energy each. A "beam screen" cooling at 10 K, intercepting the synchrotron radiation emitted by the circulating protons and the power dissipated by the beam image currents, is designed to shield the magnet cold bore. The screen will be kept during machine operation at temperatures higher than 1.9 K, in order to absorb the heat load at a lower cost. However it must be able to withstand without risk of embrittlement cooling to the magnet temperature of 1.9 K. Any ductile-fragile transition should therefore be avoided down to 1.9 K. Moreover, the screen should be totally a magnetic at cryogenic temperatures (the maximum admitted magnetic susceptibility is 5.10^{-3}). Severe conditions are imposed on the construction material of the beam screen. A quench (sudden loss of superconductivity in the magnet) will induce eddy currents in the screen which result in a risk of plastic deformation. During its life, the screen will be subjected to several thermal cycles between room temperature and cryogenic temperatures.

In the present design, the screen should have a section of 38 x 38 mm^2 and a length of about 15 m and should be longitudinally welded. To avoid a loss of magnetic and mechanical properties at low temperature, no local precipitation of the ferrite in the weld metal and in the Heat Affected Zones (HAZ) should occur. Because of their weldability and excellent austenitic stability, N2-enriched austenitic stainless steels with different Mn contents are candidate materials for the beam screen. High Mn steels are magnetically stable at low temperature.

The TIG weldability of the candidate steels is studied. The influence of welding parameters (weld speed, power ...) on the possible precipitation of delta ferrite is discussed.

CERN, MT-SM, CH-1211 Geneva, Switzerland

Il- CANDIDATE STEELS FOR THE BEAM SCREEN

The candidate N_2-enriched austenitic stainless steels for the beam screen are at the present state of the project the steel UNS 21904 produced by Ugine, 13 RM 19 by Sandvick et X20MDW by Aubert et Duval. Their compositions are given in Table 1.

The austenitic stability of the three steels may be evaluated on the basis of their position in a Hull diagram (Fig. 1). This diagram is better adapted than the traditional Schaeffler diagrams to study the austenitic stability of highly N_2-enriched steels. Hull diagram is used to estimate the ferrite content in the weld metal. Here, the effects of the various alloying elements are accounted for by use of Ni and Cr equivalents as the axes, where:

$$Cr_{eq} = Cr + 1.21\,Mo + 0.48\,Si + 2.27\,V + 0.72\,W + 2.20\,Ti + 0.14\,Cb + 0.21\,Ta + 2.48\,Al$$

$$Ni_{eq} = Ni + 0.11\,Mn - 0.0086\,Mn^2 + 0.11\,Co + 0.44\,Cu + 18.4\,N + 24.5\,C$$

The three steels are in the austenitic region of the diagram. The maximum allowed nitrogen loss (calculated on the basis of the Hull diagram) before the first precipitation of delta ferrite is reported in the last column of Tab. 1. Although the austenitic stability is not solely linked to the nitrogen content, nitrogen is a key element to keep the austenite stable in high nitrogen steels welds. Local precipitation of ferrite in austenitic steels can arise from a reduction of their nitrogen content. This property is exploited for encoding austenitic steels: local ferritic marks with soft magnetic properties can be produced by nitrogen degassing in vacuo or in Ar : a thermal treatment is applied at the surface where some regions are masked by a thin layer (Pt) while other are exposed to degassing. In the exposed regions a large ferritic precipitation occurs, in the masked regions austenite keeps stable [1].

III- EXPERIMENTAL RESULTS

The most austenitic welds could be obtained on the three steels at relatively high weld speed (> 1 m/min). Results of nondestructive testing (X-rays) show that at speeds as high as 1 m/min no gross porosity appears in the weld bead. However, welds done at a speed higher than 1.5 m/min present lacks of compactness.

An Ar/N2 shielding gas was necessary. For the steel X20 MDW and UNS 21904 nitrogen contents up to 20 % could be applied, while for the steel 13RM19 nitrogen contents in the shielding gas higher than 7 % resulted in a diffused porosity in the weld. A N_2-content of 30 % could always be applied underneath.

The weld parameters resulting in the most austenitic welds for the three steels are n ported in Tab. 2.

Microstructural investigations show that the size of the weld bead and the HAZ depend on the energy deposited during welding (and in particular on the weld speed, the nitrogen content in the shielding gas and the energy associated with the weld). High welding speed results in a narrow weld bead and a HAZ low in ferrite (example in Fig. 2).

However, delta ferrite could never be totally avoided in the HAZ. The crown of the HAZ was always almost fully austenitic, while some ferrite precipitated in spots at the root, where an extended recrystallisation occurs. A typical ferrite precipitation in the HAZ is shown in Fig. 3. The use of a heat shunt does not generally improve the austenitic stability. Only for the steel 13RM19 the heat shunt allowed to reduce the root ferrite.

A carbide dissolution is typically observed in the HAZ of the steel 13RM19, containing relatively high carbon (Tab. 1). Less energy is sufficient for carbide dissolution compared to recristallisation or ferrite precipitation.

IV- **INTERPRETATION AND DISCUSSION OF THE EXPERIMENTAL RESULTS**

The choice of suitable welding parameters is capital to avoid ferrite precipitation. The critical parameters to be controlled are:

- the composition of the shielding gas, and in particular its nitrogen content;
- the welding speed
- the energy carried by the arc

A suitable composition of the shielding gas allows to keep the weld bead fully austenitic. An increased welding speed allows to reduce the precipitation of delta ferrite in the HAZ. The energy density (Φ received by the material per unit of melted surface may be expressed as (see Fig. 4) :

$$\Phi = \frac{Wdt}{2\rho dx} = \frac{W}{2\rho v} \qquad (1)$$

where ρ is the half size of the weld bead, ν the welding speed and W the energy carried by the arc. The relation holds supposing that the energy is solely applied to the melted region. High speed allows to reduce the energy density at constant W. However, the welding will be possible only if W increases with the welding speed. (Φ should be large enough for a good penetration. The more austenitic TIG welds were obtained at an energy density between 14 (X20MDW) and 28 J/mm^2 (13RM19), corresponding to energies higher compared to the energy necessary to heat the metal up to the melting point and to melt it.

Nevertheless, at a given W, a high ν allows the ferrite content in the HAZ to be minimised. The ferritic regions in the HAZ- are always adjacent to the melt metal. Delta ferrite precipitates when the base metal adjacent to the melt remains at a temperature comparable to the melting temperature ($T \leq T_f$). Let us consider as in Fig. 5 a point A near the melted bead. If we suppose that the melted zone has approximately a square section, the time spent by the

critical temperature $T \leq T_f$ (melting temperature) can be estimated at $2\rho/v$. It is known that in the equation for the heat diffusion:

$$\frac{\partial T}{\partial t} = D\frac{\partial^2 T}{\partial x^2} \qquad (2)$$

(where D is the coefficient of thermal diffusion) the characteristic distance x where T reaches a given and constant value is[1] [2] : $x \propto \sqrt{Dt}$. We take $t = \tau(= 2\rho v)$ The temperature range where the delta ferrite is stable in the phase diagram will depend on the steel composition. The extent of the ferritic precipitation is linked to x. Evaluating for every weld the critical time t and the depth of the ferritic precipitation in the HAZ, we find that x is proportional to $\sqrt{\tau}$, i.e to $\sqrt{1/v}$.

Let us now quantitatively estimate the width of the thermally destabilized region. For several austenitic stainless steels one finds out a value of D at 1400°C of about $(5.5 \pm 0.5)\ 10^{-6}$ m^2/s[3] For the initial condition (Fig. 5) t=0, x>0 (in the base metal), TO=T,,, (for a large enough piece) and the boundary condition $t>O,\ x=0$ (beside the weld bead), T=Tf, the solution of the equation (2) is :

$$\frac{T - T_f}{T_{room} - T_f} = Erf(x / 2\sqrt{D\,t}) \qquad (3)$$

Assuming as $T\text{-}T_f$ the temperature range where the ferrite delta is stable in the phase diagram (about 100°C), we find for a 13 RM 19 steel welded at 0.24 m/min a depth of the destabilized region of about 200 μm. The observed depth of the ferrite is 100 μm at the crown of the HAZ and is then comparable to the size of the estimated thermally destabilized region. Repeating for the other welds the same evaluation, one observes that the ferrite penetration is less extended than the thermally destabilized region. The delay due to the kinetics of the precipitation of the delta phase may be the basis for this difference.

On the other hand, low welding speed will not be sufficient to the dissolution of the phase δ, as it is experienced in the low speed welds. In the steels solidifying in the delta phase, and in the double steels, the works of Hoffmeister [4] and Mundt et Hoffmeister [5] suggest that δ can dissolve by a very slow cooling. As well, in the steels with a very low ferrite content, the ferrite dissolve on times much longer than the times involved in a welding operation. The works of Lee and Dew-Hugues [6] show that long times and elevated temperatures are necessary to dissolve delta ferrite: a heat treatment at 1000°C during 1/2 h has no effect on the ferrite content of an austenitic steel. Times of 10 h at 1050°C are necessary to have a full dissolution [7] The precipitation of delta can then be reduced only by a high speed welding.

The present discussion also explains why Electron Beam welding (EB) maintains a fully austenitic structure in the same steels. HAZs are absent. The size of the weld bead is smaller in EB compared to TIG for similar welding speeds. As the size of the weld bead appears at

[1] For special initial and boundary conditions, which are well verified in our case.

denominator in the expression of τ, EB welding results in "critical" times up to 400 times shorter compared to TIG (Tab. 3).

V- CONCLUSIONS

The TIG weldability of the three candidate steels for the beam screen of LHC was studied. Welds with a reduced ferritic content could be obtained through a strict control of the welding parameters : composition of the shielding gas, power, welding speed.

The relationship between welding parameters and ferrite precipitation was studied. The extent of delta ferrite precipitation depends on the time spent by HAZ in the critical temperature range of ferrite precipitation. The extent of this range depends on the steel composition. The appropriate choice of the welding parameters (in particular the welding speed) allowed to reduce the delta ferrite precipitation to some isolated spots at the root of the HAZ and to obtain an almost totally austenitic crown.

VI- ACKNOWLEDGEMENTS

The authors are indebted to S. Marque and J. Haffner for their help in microstructural observations, to C. Margaroli for the non-destructive testings, M. Caccioppolli and T. Tardy for performing the welds. Thanks are due to A. Poncet for proposing the subject and to C. Benvenuti for the critical review of the manuscript.

VII- BIBLIOGRAPHY

[1] Feichtinger H., Piazza D., *Functional Nitrogen Steels,* Proceedings of the 1st Swiss Conference on Materials Research for Engineering Systems, 8-9 Sept. 1994, Sion, Switzerland

[2] Bénard J. et al., *Métallurgie générale,* Masson, Paris (1984)

[3] Peckner D. et Bernstein I.M., *Handbook of Stainless Steels,* Mc Graw Hill, New York (1977)

[41 Hoffmeister H. : K*ristallseigerungen und Deltaferritbildung in austenitischem Schweissgut,* DVS-Bericht Nr 3, 2-8 (1973)

[5] Mundt R. et Hoffmeister H. : The *Continuous Delta-Gamma Transformation During Cooling of Ferritic-austenitic Iron-Chromium-Nickel Alloys,* Arch. Eisenhiittenwes. 54 333 (1983)

[61 Lee K.S. et Dew-Hugues D., *Effect of EB Welding and Cold Rolling on Low Temperature strength and Toughness of Austenitic Stainless Steels,* in: Austenitic Steels at Low Temperatures, Reed R.P. et Horiuchi T. eds., New York (1983)

[71 Peckner D. et Bernstein I.M., *Handbook of Stainless Steels,* Mc Graw Hill, New York (1977)

acier	Cr	Mo	Si	Ni	Mn	N	C	Cr-eq	Ni-eq	allowed N_2 loss (ppm)
13 RM 19 (S)	18.5		0.8	7	6	0.25	0.11	18.88	14.64	*666*
UNS 21904 (U)	20			7	9	0.38	0.03	20	15.02	*395*
X20MDW (A)	20.35	2.12	0.4	9.57	3.97	0.366	0.034	23.10	17.43	*201*

Tab. 1 : Composition of selected steels for the beam screen of the LHC

Tab. 1: Composition des aciers à *1'étude*

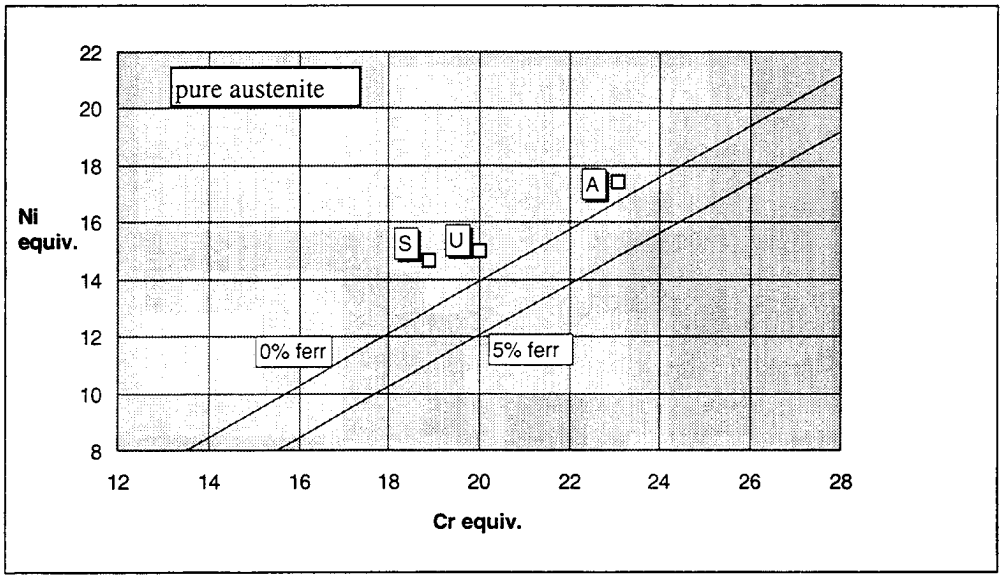

Fig. 1: Hull diagram for determining the approximate amount of δ-ferrite in the microstructure of austenitic stainless steel welds. The candidate steels are fully austenitic.

Fig. 1 : Diagramme de Hull. Les lignes continues représentent la teneur en ferrite dans un diagramme N_{iq}-$Cr_{éq}$. Les trois aciers se trouvent en Zone complètement austénitique.

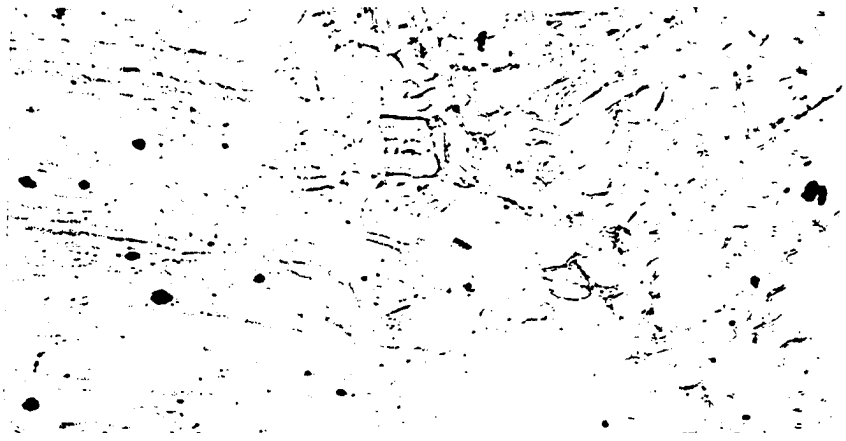

Fig. 2 Microstructure of 13RM19 steel (crown of the HAZ), welded under 7% N_2 at the speed of 60 cm/min

Fig. 2 : Microstructure (ZAT, côté couronne) relative à *l'acier 13RM19, soudé sous protection de 7% d'N_2,à la vitesse de 60 cm/min.*

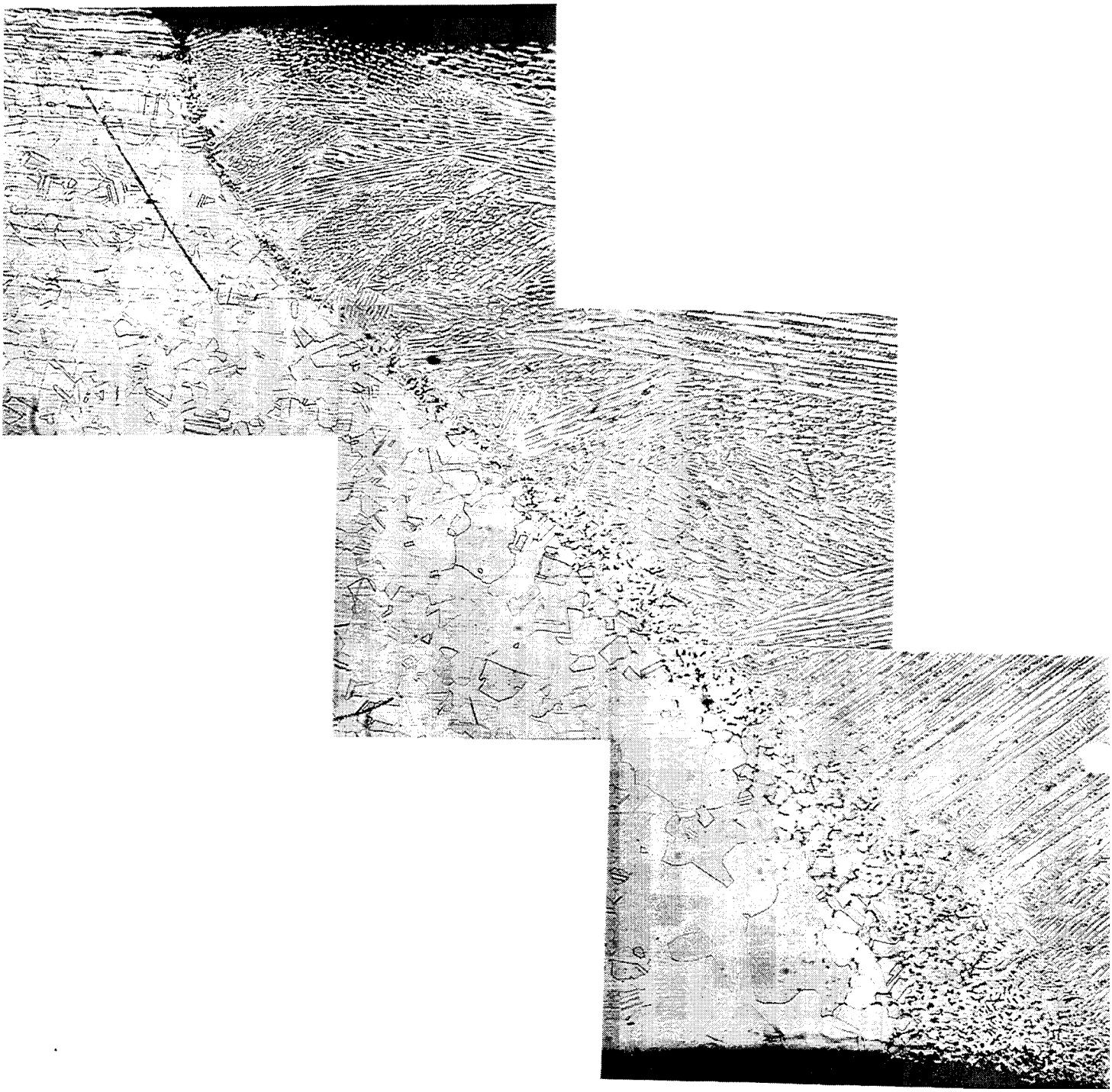

Fig. 3: HAZ of the steel UNS21904, welded under 15%N2 (speed: 100 cmlmin)

Fig. 3 : Microstructure (ZAT) relative b Vacier UNS 21904, soudé sous protection de 15% N_2, à *la vitesse de 100 cm/min.*

	shielding gas	*speed (cm/min)*	*gas flux (l/min)*	*bead size (mm)*	*extent of ferrite in HAZ*
13RM19	Ar 93%-N_2 7%	60	20	0.4 (c)- 2 (r)	60 µm
UNS 21904	Ar 80%-N_2 20%	100	20	1.4 (c) - 2.9 (r)	20 à 140 µm
X20MDW	Ar 80%-N_2 20%	125	20	0.9 (c) - 2.8 (r)	traces

Tab. 2 Optimized welding parameters

Tab. 2 Paramètres de soudage optimisés pour les trois nuances, correspondant au minimum de précipitation ferritique

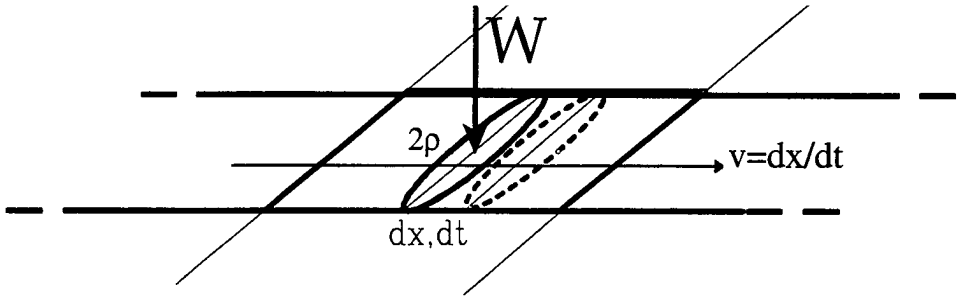

Fig. 4 : Energy deposited during welding

Fig. 4 : Dépôt d'énergie pendant l'avancement du soudage

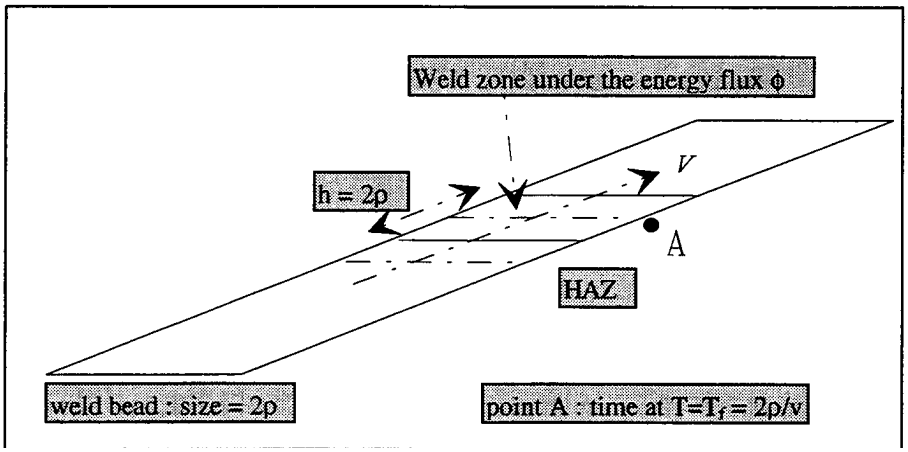

Fig. 5 : Thermal destabilisation of a point A adjacent to the molten metal (see text). h (≅ 2ρ) is the size of the melted metal in the direction of weld bead.

Fig. 5 : Le temps de permanence d'un point à une température voisine de la température de fusion dans la ZAT (près de la zone en solidification) dépendra inversement de la vitesse d'avancement. h (≅ 2ρ) est la taille de la zone fondue dans la direction d'avancement.

	weld speed v (cm/min)	*bead size 2ρ (mm)*	*critical time τ=2ρ/ v (ms)*
TIG	6 to 125	1.2 to 3.5	130 to 3000
EB	100 to 250	0.31 to 1	7 to 40

Tab. 3 : Critical times for the precipitation of δ-ferrite involved by the two techniques TIG and EB

Tab. 3 : Comparaison des temps critiques pour la précipitation de la ferrite delta mis en jeu par les deux techniques.